PNAS RESEARCH ARTICLE | CELL BIOLOGY

KAT8-catalyzed lactylation promotes eEF1A2-mediated protein synthesis and colorectal carcinogenesis

Bingteng Xie[a,1], Mengdi Zhang[b,1], Jie Li[c,d,1], Jianxin Cui[e], Pengju Zhang[b], Fangming Liu[b], Yuxi Wu[f], Weiwei Deng[b], Jihong Ma[c,d], Xinyu Li[c,d], Bingchen Pan[a], Baohui Zhang[g], Hongbing Zhang[b], Aiqin Luo[a], Yinzhe Xu[h,2], Mo Li[c,d,2], and Yang Pu[b,2]

Edited by Mohammad Kamran, University of Illinois at Urbana Champaign, Champaign, IL; received August 23, 2023; accepted December 18, 2023 by Editorial Board Member Katherine A. Fitzgerald

Aberrant lysine lactylation (Kla) is associated with various diseases which are caused by excessive glycolysis metabolism. However, the regulatory molecules and downstream protein targets of Kla remain largely unclear. Here, we observed a global Kla abundance profile in colorectal cancer (CRC) that negatively correlates with prognosis. Among lactylated proteins detected in CRC, lactylation of eEF1A2K408 resulted in boosted translation elongation and enhanced protein synthesis which contributed to tumorigenesis. By screening eEF1A2 interacting proteins, we identified that KAT8, a lysine acetyltransferase that acted as a pan-Kla writer, was responsible for installing Kla on many protein substrates involving in diverse biological processes. Deletion of KAT8 inhibited CRC tumor growth, especially in a high-lactic tumor microenvironment. Therefore, the KAT8-eEF1A2 Kla axis is utilized to meet increased translational requirements for oncogenic adaptation. As a lactyltransferase, KAT8 may represent a potential therapeutic target for CRC.

lactylation | protein synthesis | colorectal cancer | lactyltransferase

Lactate is a by-product of aerobic glycolysis (Warburg effect) but has also been reported to play a role in epigenetic modification (1). It acts as a precursor leading to the addition of lactyl groups to the ε-nitrogen of a lysine side chains in protein substrates named lysine lactylation (Kla), in particular on histones. Kla directly modulates gene transcription from chromatin. Physiologically, histone modified by Kla has been shown to be involved in immune cell homeostasis (2, 3), stem cell differentiation, and early embryonic development (4). Pathologically, elevated histone Kla modification is correlated with ulcerative colitis (2), lung fibrosis (5), sepsis (6), systemic lupus erythematosus, and ocular neoplasm (7). Most studies reporting about Kla are limited to the nucleus, especially on histones related to balancing the gene transcriptional activation and suppression, thereby contributing to disease initiation and development. Although emerging evidence has shown the existence of Kla on a diverse spectrum of cellular proteins by profiling the whole lactylome in hepatocellular carcinoma (8, 9), few are focused on the underlying mechanisms of cellular functional changes mediat (ed by lactylation. Functional studies of Kla-modified proteins or pathways require knowledge of their catalytic enzymes (writers and erasers) and substrates. It is found that overexpression or depletion of the acyltransferase p300 can increase or decrease histone Kla levels in cells, indicating that p300 is a potential histone Kla writer (1). Screening of 18 mammals' lysine deacetylases has revealed that histone deacetylase 1-3 have delactylase capacity to remove Kla from histones (10). Despite these findings, little is known about the regulatory elements of global lactylation.

Lactate release in malignancies is significantly increased as compared to peripheral tissue (11). Excess lactate creates an acidic tumor microenvironment (TME) due to enhanced glycolysis metabolism in tumors. High concentrations of lactate are positively correlated with nodal or distant metastases and poor survival in various cancers (12). Lactate promotes tumor growth in multiple ways, not only by representing an energy source for tumor cells but also by reprogramming the TME. On one hand, lactate can be directly absorbed and metabolized by tumor cells to fuel the TCA cycle and regulate hypoxia responses and mitosis (13). On the other hand, lactate has been reported to create an immunosuppressive TME by repolarizing tumor-associated macrophages, up-regulating PD-1 on T cells, and inhibiting antigen presentation on dendritic cells (14). The identification of lactylation further broadens and highlights the role of lactate in oncogenesis. Kla could act as a crucial bridge connecting tumor metabolism, cancer development, and potential patient outcome.

Elongation factor 1 alpha (eEF1A) is one of the most abundant and evolutionarily conserved proteins in the eukaryotic proteome (15). As a regulator of translational elongation, eEF1A promotes the binding of ribosomes to aminoacyl tRNA during protein synthesis

Significance

Lysine lactylation (Kla) is a posttranslational modification that links cellular metabolism to epigenetic regulation. This is relevant for many tumors that thrive in an acidic environment containing high levels of lactic acid due to excessive glycolysis. Through the protein lactylome analysis of human colorectal cancer tissues and cancer cell lines, we identified the translation initiation factor eEF1A2 (Elongation factor 1 alpha) to be hyperlactylated, leading to enhanced translation activity. The eEF1A2 lactylation-mediated increase in protein synthesis contributes to oncogenic adaptation. Additionally, we identified a lactyltransferase, KAT8, among the eEF1A2-interacting proteins, capable of lactylating multiple oncogenic proteins. Our study may pave the way for a strategy to suppress cancer cells within the high-lactic tumor microenvironment by employing KAT8 inhibitors.

Preprint Servers: The earlier version of this manuscript has been uploaded onto the preprint platform-Research Square on Oct.2022, DOI:10.21203/rs.3.rs-2177254/v1.

The authors declare no competing interest.

This article is a PNAS Direct Submission. M.K. is a guest editor invited by the Editorial Board.

[1]B.X., M.Z., and J.L. contributed equally to this work.

[2]To whom correspondence may be addressed. Email: puyang_py@163.com, limo@hsc.pku.edu.cn, or james_hbp@163.com.

This article contains supporting information online at https://www.pnas.org/lookup/suppl/doi:10.1073/pnas.2314128121/-/DCSupplemental.

Published February 15, 2024.

(16). There are two isoforms of eEF1A in mammalian cells, eEF1A1 and eEF1A2, which possess 98% similarity in amino acid levels but show different expression patterns. It is known that eEF1A2 involves in tumorigenesis and cancer development (17). Reactivation of eEF1A2 stimulates phospholipid signaling and promotes Akt-dependent cell migration and actin remodeling that ultimately favors tumorigenesis (18, 19). Moreover, eEF1A2 promotes tumor progression via posttranslational modification (PTM) (15). For instance, eEF1A2 methylation serves as a mechanism employed by malignancies to adapt to their augmented translational requirements (20). Since PTMs are efficient and low-cost approaches to govern protein function, it is interesting to examine whether there are other PTMs involved in eEF1A2-mediated oncogenic regulation.

In this study, we observed up-regulated global Kla levels in CRC (colorectalcancer), which associated with poor disease prognosis. Among the CRC lactylome profile, we revealed eEF1A2 lactylation contributing to elevated protein synthesis, thereby facilitating tumor growth. By exploring regulators of the eEF1A2 lactylation, KAT8 was identified as a global lactyltransferase. Given that many KAT8-catalyzed Kla substrates located within tumorigenic pathways, genetical and pharmacological depletion of KAT8 significantly decreased global Kla levels and inhibited tumorigenesis in the CRC mouse model with a high-lactic (LA) TME. Our data uncovered a Kla-mediated mechanism of tumor adaptation to aberrant translational necessities and identified KAT8 as a Kla writer that could be targeted in cancer treatment.

Results

Elevated Global Lactylation is Associated with an Unfavorable Prognosis for Tumor Progression and CRC Patients. The Warburg effect is a hallmark of cancer (21). Its by-product lactate has been considered as a prognostic indicator for CRC patients (22–24). Since lactate has been recently considered as a substrate for protein Kla, we explored the relevance of Kla to tumor development and patient prognosis. We checked global Kla levels in CRC tissues and their clinical correlation by performing multiple immunofluorescence (IF) staining analysis of a tissue microarray (TMA) consisting of 100 CRC cases (Fig. 1*A* and *SI Appendix*, Fig. S1*A* and Table S1). Higher global Kla level in tumors was correlated with the aggressiveness of cancer and patient poor prognosis (Fig. 1 *B* and *C*). Furthermore, we found increased global Kla presented in tumor samples compared to the adjacent normal tissues (Fig. 1 *D* and *E* and *SI Appendix*, Table S2). In concert with the observation in human tissues, global Kla levels were higher also in CRC cell lines (CACO2, HCT116, LS174T, SW480, and LOVO) than in nontransformed intestinal epithelial cell lines (NCM460 and CCD841) (Fig. 1*F*). Together, these data suggest a potential link between increased global Kla levels and CRC pathogenesis.

We then explored whether tumorigenic Kla levels depended on intracellular lactate levels. Glycolysis inhibitors (2 deoxy-D-glucose (2-DG) and dichloroacetate (DCA)) significantly reduced intracellular lactate production and global Kla levels in a dose-dependent manner in CRC cells (Fig. 1*G* and *SI Appendix*, Fig. S1*B*). Correspondingly, glycolysis inhibitors suppressed CRC cell proliferation (Fig. 1*H*). Given that 2-DG and DCA may exert other effects to cells except for suppressing lactate production and regulating Kla levels, we tried to simultaneously silence LDHA and LDHB to attenuate lactate production in HCT116 cells (*SI Appendix*, Fig. S1*C*). Decreased intracellular lactate production by silencing LDHA and LDHB led to reductions of cellular proliferation and Kla levels while adding sodium lactate (NaLa) to the cell culture system could replenish the reduced cellular proliferation and Kla levels (*SI Appendix*, Fig. S1 *D* and *E*). These findings indicate that lactylation involves in the mechanism by which lactate regulates cell proliferation. We further examined the localization of Kla-modified proteins in human tumor samples and CRC cell lines and found lactylated proteins existed not only in the nucleus but also in the cytoplasm (Fig. 1 *I*–*K*). These results signify that lactate production is a key determinant of Kla, and elevated lactylation may contribute to CRC tumorigenesis and progression.

eEF1A2 Is Hyperlactylated in CRC. To reveal the lactylated proteins in CRC, we analyzed the lactyl-proteome of seven paired biopsies derived from CRC patients using tandem mass spectrometry analysis (LC–MS/MS) (25). A wide protein lactylation landscape of 1,254 sites were detected in 1,230 modified peptides belonging to 859 proteins (Fig. 2*A* and Dataset S1). Notably, Kla-modified proteins not only confined to the nucleus but also to the cytoplasm, mitochondrion, and the endoplasmic reticulum. This distribution suggested that in addition to the well-known modification on histones, Kla also targets nonhistone substrates in various cellular compartments (Fig. 2*B*). Gene ontology (GO) enrichment and Kyoto Encyclopedia of Genes and Genomes (KEGG) analysis further confirmed that Kla functioned broadly by modifying proteins in both the nucleus and cytoplasm (*SI Appendix*, Fig. S2 *A* and *B*).

Various up-regulated and down-regulated protein lactylation sites were observed in cancer tissues as compared to normal tissues (Fig. 2*C*). We performed GO enrichment analysis among them to determine the roles of these differentially lactylated proteins. Notably, many up-regulated-lactylation protein sites were found to be involved in translation, indicating that Kla may regulate protein synthesis in CRC (Fig. 2*D*). A strong colocalization between Kla and ribosome complexes where RNA was translated into protein also provided supportive evidence to this inference (*SI Appendix*, Fig. S2*C*). Using the Search Tool for the Retrieval of Interacting Gene/Proteins (STRING) database (26), we visualized protein–protein interaction networks among the differentially lactylated proteins (Fig. 2*E*). Considering the differential levels of lactylated proteins between tumor and para tissues as well as the protein–protein interaction networks involving proteins regulating translation, we thus focused on the lactylation of eEF1A2 ($\log_2$ fold change 1.97, $P < 0.05$), a classical mRNA translation factor, to investigate how Kla may modulate protein translation, potentially relevant for CRC pathology.

To this end, we performed ex vivo validation of eEF1A2 lactylation from the CRC lactylome data. IF staining showed colocalization of the Kla modification and eEF1A2 in CRC cells (Fig. 2*F*). Immunoprecipitation (IP) of endogenous and exogenous eEF1A2 was performed in cellular extracts from wild-type or Flag-eEF1A2-expressed CRC cell lines with anti-eEF1A2 and anti-Flag antibody, followed by WB with an antibody against pan-Kla. We detected strong lactylation of both exogenous and endogenous eEF1A2 in CRC cells in the presence of NaLa (Fig. 2 *G*–*I*). In accordance with the IF staining, these data further confirmed the occurrence of lactylated eEF1A2 in CRC cells.

Lactylation of eEF1A2 Promotes Tumor Cell Proliferation. LC–MS/MS analysis of CRC biopsies revealed that lysine residue 408 was the major lactylation site of eEF1A2 (Fig. 3*A*). Sequence analysis of eEF1A2 implicated that K408 was a highly conserved site from *Saccharolobus solfataricus* to Homo sapiens (*SI Appendix*, Fig. S3*A*). Because arginine (R), as a conservative substitute to K, may cause minimal structural change and retain positive charge, the K-R mutations are commonly used to mimic lysine

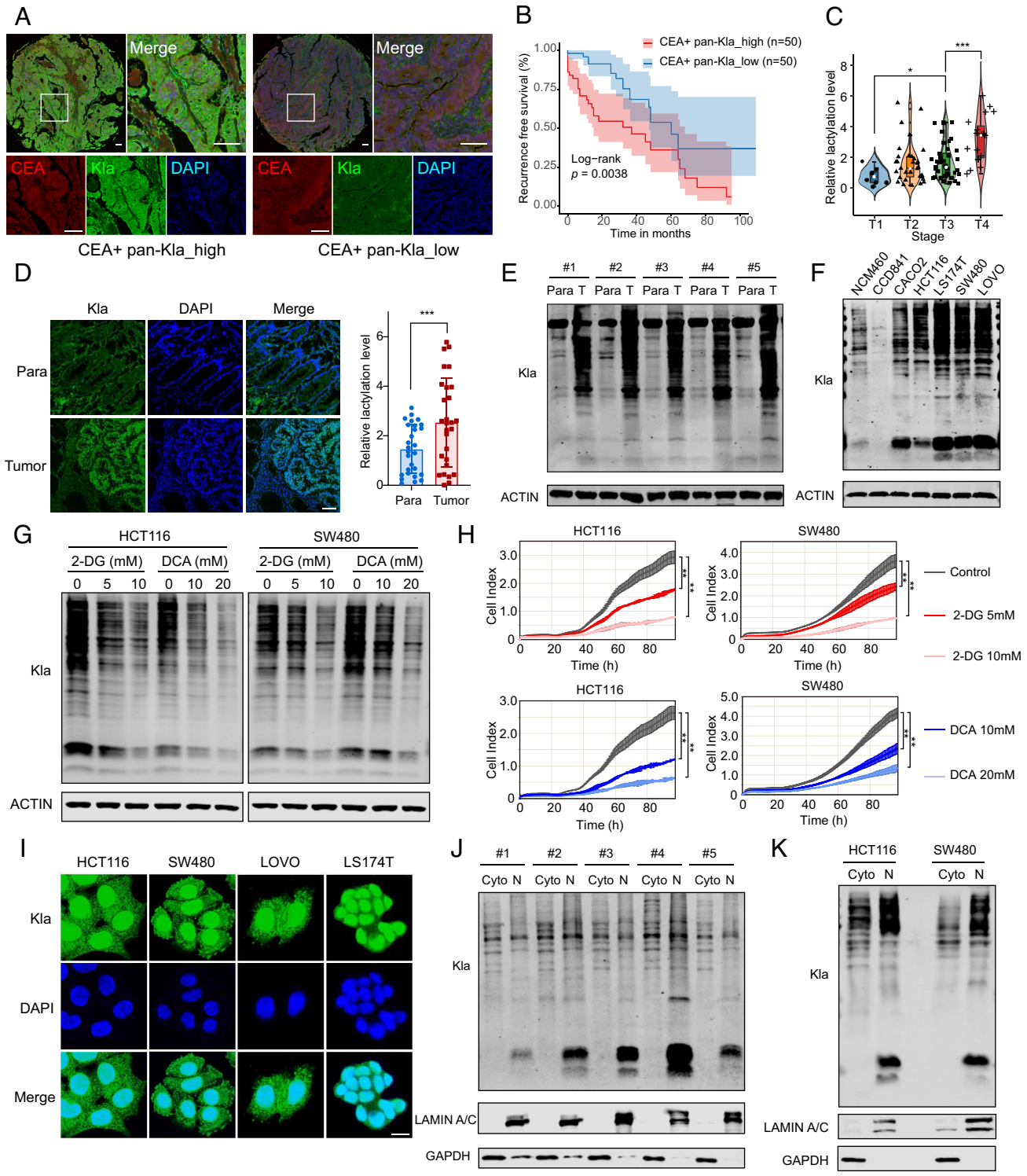

Fig. 1. Elevated global lactylation is associated with an unfavorable prognosis for tumor progression and CRC patients. (*A*) Representative multiplexed immunostaining images of pan-Kla and CEA in CRC. (Scale bars, 100 μm.) (*B*) Kaplan–Meier curves of time for recurrence-free survival showing the difference between CRC patients with low and high Kla levels. n = 100. The log-rank *P* value is denoted for differences. (*C*) Kla levels in patients at American Joint Committee on Cancer (AJCC) stages T1 to T4; n = 100. (*D*) Representative IF staining for Kla in paired CRC samples; n = 28. (Scale bar, 100 μm.) The *Right* panel represents relative Kla levels quantified using ImageJ. Para, para-carcinoma tissue. (*E*) Kla levels were detected in Para and tumor tissues (T) by western blotting (WB). (*F*) Kla levels were detected in intestinal cell lines and CRC cell lines by WB. (*G*) Kla levels were detected in HCT116 and SW480 cells treated with different concentrations of 2-DG or DCA for 24 h by WB. (*H*) Real-time cell proliferation assay of HCT116 and SW480 cells treated with different concentrations of 2-DG or DCA for 96 h. (*I*) Kla levels were detected in CRC cell lines by IF staining. (Scale bar, 10 μm.) (*J*) Cellular fractionations of CRC patients' colonic tissues were analyzed by WB; Cyto, cytoplasm; N, nuclear. (*K*) Cellular fractionations of HCT116 and SW480 cells were analyzed by WB. **P* < 0.05; ***P* < 0.01; ****P* < 0.001. Analyses were performed using unpaired, two-tailed Student's *t* test (*C*, *D*, and *H*). Data are shown as means ± SD.

acylation defects (27–29). To examine whether K408 was the main lactylation site of eEF1A2, we created a protein delactylated mimetic of eEF1A2 by mutating the site 408 from K to R and found the K408R mutant resulted in significantly decreased Kla especially in the presence of NaLa (Fig. 3*B*). We further examined whether the K-R mutation at the 408 site herein altered the

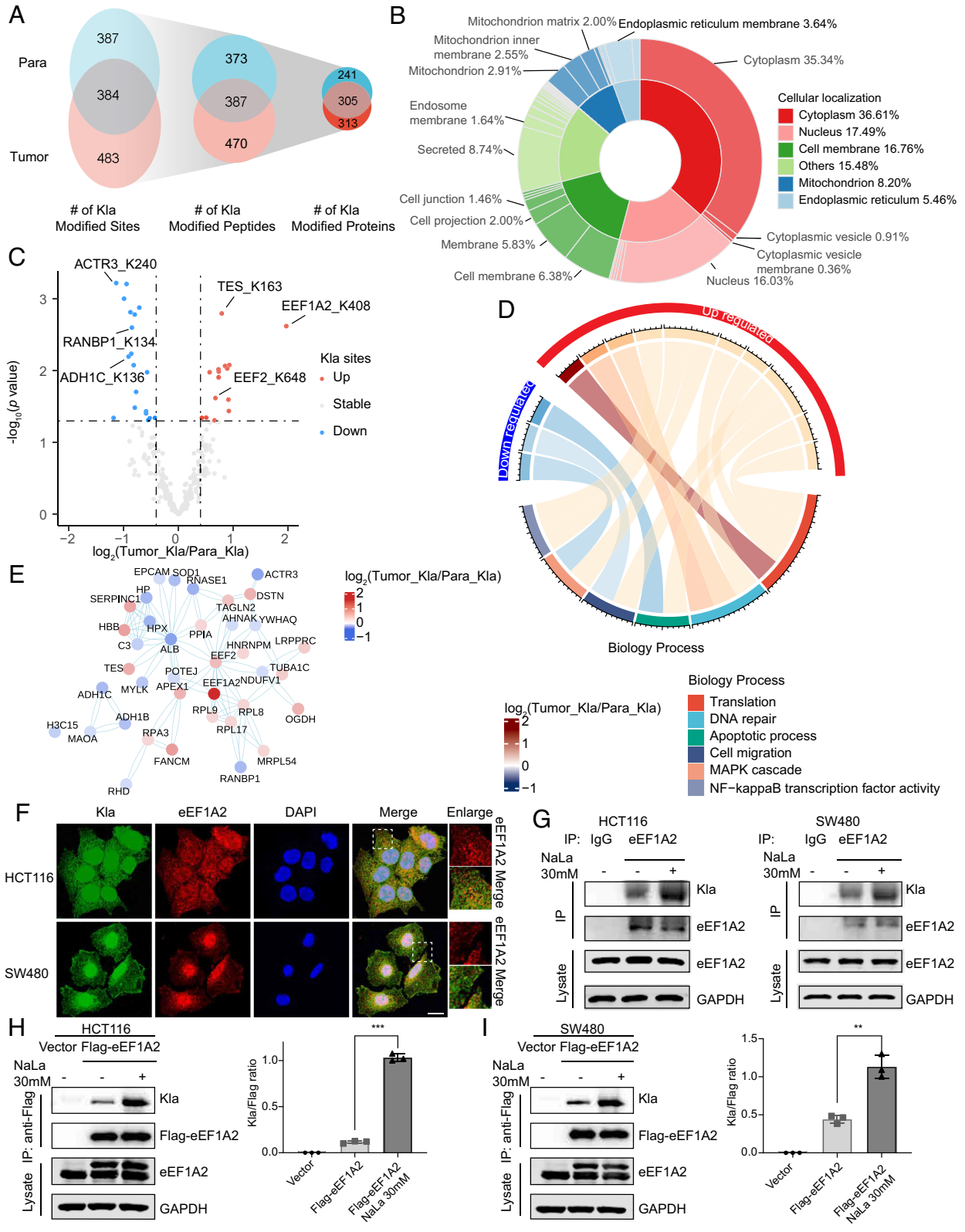

Fig. 2. eEF1A2 is hyperlactylated in CRC. (*A*) The number of Kla-modified sites, peptides, and proteins identified from CRC patient samples. (*B*) Sunburst chart representing the subcellular distribution of Kla-modified proteins. (*C*) Volcano plot showing the lactylome changes in CRC tissues compared to the adjacent normal tissues. (*D*) Chord plot showing the relationship between up-regulated and down-regulated Kla-modified protein sites identified from differentially lactylated proteins between CRC tumor and adjacent normal tissues in GO terms of biology processes. (*E*) Protein–protein interaction network of differentially lactylated proteins between CRC tumor and adjacent normal tissues based on the STRING database. (*F*) Representative IF staining for Kla and eEF1A2 in HCT116 and SW480 cells. (Scale bar, 10 μm.) (*G*) Endogenous Kla levels of eEF1A2 in HCT116 and SW480 cells. eEF1A2 Kla level was analyzed by immunoprecipitation (IP) with an anti-eEF1A2 antibody followed by WB for Kla. (*H* and *I*) Kla levels of eEF1A2 in HCT116 (*H*) and SW480 (*I*) cells stably expressing Flag-eEF1A2 with or without NaLa. The whole cell lysates (WCE) were used for IP with an anti-Flag antibody, followed by WB for Kla. The *Right* panel represents WB quantification. Data are shown as means ± SD, $^{**}P < 0.01$, $^{***}P < 0.001$; unpaired, two-tailed Student's *t* test.

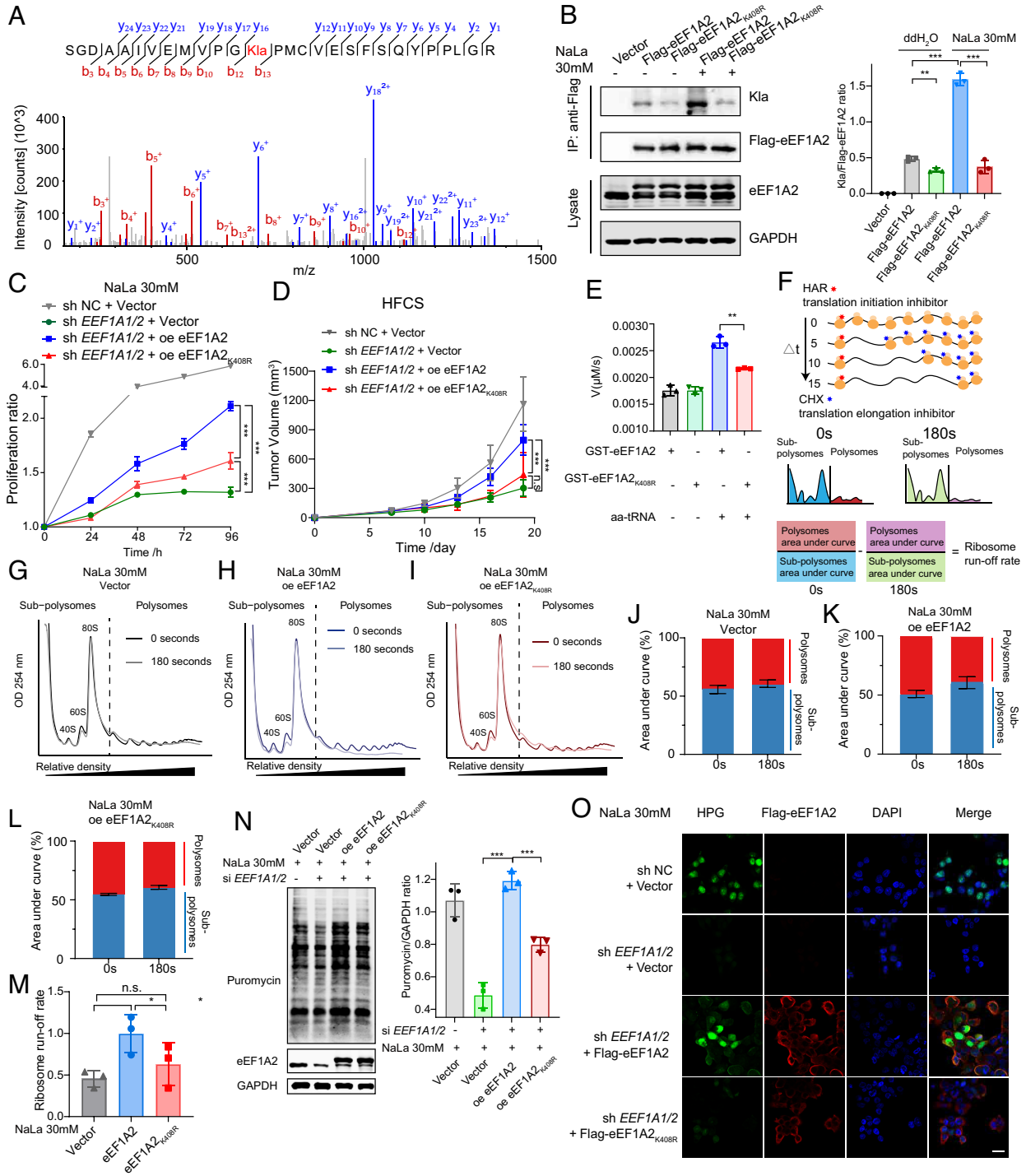

Fig. 3. Lactylation of eEF1A2 enhances protein synthesis and tumor cell proliferation. (*A*) MS/MS spectra of the lactylated eEF1A2 peptide for the identification and quantification of K408 lactylation on eEF1A2. b and y ions indicate peptide backbone fragment ions containing the N and C termini, respectively. Lactylated lysine is colored in red. (*B*) Kla levels of eEF1A2 in HCT116 cells stably expressing Flag-eEF1A2 or Flag-eEF1A2$_{K408R}$ with or without NaLa. The WCE were used for IP with an anti-Flag antibody, followed by WB for Kla. The *Right* panel represents WB quantification. (*C*) Cell proliferations of control (sh NC plus control vector) or EF1A1/2-depleted HCT116 cells overexpressed (oe) with control vector or wt-eEF1A2 (eEF1A2) or delac-eEF1A2 (eEF1A2$_{K08R}$) in the presence of NaLa were measured with cell count proliferation assay. (*D*) Tumor growth curves for mice (n = 5/group) fed with HFCS bearing control (sh NC plus control vector) or eEF1A1/2-depleted HCT116 cells overexpressed with control vector or wt-eEF1A2 or delac-eEF1A2. (*E*) Velocity of phosphate formation of lactylated or delactylated GST-eEF1A2 in GTP hydrolysis assay. (*F*) Schematic diagram of Harringtonine run-off assay. (*G–I*) Representative polyribosome profiles from control vector (*G*) or wt-eEF1A2 (*H*) or delac-eEF1A2 (*I*) overexpressed HCT116 cells in the presence of NaLa treated with harringtonine for 0 s and 180 s before harvest. (*J–L*) The areas under curve of control vector (*J*) or wt-eEF1A2 (*K*) or delac-eEF1A2 (*L*) overexpressed HCT116 cells in the presence of NaLa under the subpolysome (40S, 60S, and 80S). Polysome sections were quantified and expressed as a percentage of their sum. (*M*) Ribosome run-off rates of control vector or wt-eEF1A2 or delac-eEF1A2-overexpressed HCT116 cells in the presence of NaLa. This run-off rate represents the shift in S:P between the two time points, which is proportional to elongation speed. (*N*) Protein production levels were detected by SUnSET assays in control (si NC plus control vector) or eEF1A1/2-depleted HCT116 cells overexpressed with control vector or wt-eEF1A2 or delac-eEF1A2 in the presence of NaLa. The *Right* panel represents WB quantification. (*O*) HPG incorporation assay in control (sh NC plus control vector) or eEF1A1/2-depleted HCT116 cells overexpressed with wt-eEF1A2 or delac-eEF1A2 in the presence of NaLa. (Scale bar, 20 μm.) *P < 0.05; **P < 0.01; ***P < 0.001; n.s., no significance. Analysis was performed using unpaired, two-tailed Student's t test (*B*, *E*, *M*, and *N*) and two-way ANOVA (*C* and *D*). Data are shown as means ± SD.

protein structure of eEF1A2 (Uniprot. Q05639). We predicted the structure of eEF1A2K408R mutation using AlphaFold (*SI Appendix*, Fig. S3 *B*, *Middle*, light green). We superimposed the different eEF1A2 structures (with or without K408R mutation) onto the mammalian ribosomal elongation complex (PDB: 5LZS) and compared the mutant structure with the original one. We found that there were no gross conformational changes between these two structures (*SI Appendix*, Fig. S3 *B*, *Right*). The root mean square deviation, which is a popular measure of structural similarity between protein structures, is 0.8 Å, also indicating the highly similarity of these two structures. There is another cryo-EM structure of extended eEF1A2 bound to the ribosome in the classical pre+ state (PDB: 8B6Z). The cryo-EM structure of this complex revealed that the K408 site of eEF1A2 in the classical pre+ state located on the protruded side chain (*SI Appendix*, Fig. S3*C*), which suggested that the K-R mutation at this site may not alter the overall configuration as well. Besides R, we explored alanine (A) for K408 mutation and found that the K408A variant yielded similar results as compared to K408R (*SI Appendix*, Fig. S3*D*). Considering the high similarities in charges and structures between K and R while the significant differences in side chain properties between K and A, K408R mutation was used for mimicking eEF1A2 delactylation in the subsequent functional experiments.

We then examined whether the up-regulated lactylation of eEF1A2K408 (eEF1A2K408la) in cancer cells has a potential role in oncogenesis. We first depleted endogenous eEF1A1 and eEF1A2 to avoid mutual compensation of the eEF1A isoforms in HCT116 cells and found that the depletion reduced cellular proliferation. Exogenous expressions of either wild-type eEF1A2 (wt-eEF1A2) or delactylated $eEF1A2_{k408R}$ mutant (delac-eEF1A2) modestly potentiated the proliferation of eEF1A1/2-depleted HCT116 (HCT116-sh eEF1A1/2) cells under normal culture conditions (*SI Appendix*, Fig. S3*E*). In the presence of NaLa, overexpression of wt-eEF1A2 significantly restored the compromised eEF1A1/eEF1A2-depleted cell proliferation, whereas overexpression of delac-eEF1A2 had only moderate impact on cell proliferation regardless of lactic conditions (Fig. 3*C* and *SI Appendix*, Fig. S3*E*). To assess the oncogenic role of eEF1A2K408la in vivo, we subcutaneously injected HCT116-sh eEF1A1/2 ± wt/delac-eEF1A2 cells into nude mice fed with high fructose corn syrup (HFCS) (*SI Appendix*, Fig. S3*F*). It is reported that HFCS administration can be used to create a high-LA TME in vivo (30). And we did observe increases in tumoral lactate levels in mice fed with HCFS (*SI Appendix*, Fig. S3*G*). Consistent with observations in vitro, reduced tumor development of eEF1A1/2-depleted cells was only restored by overexpression of wt-eEF1A2, but not delac-eEF1A2 in mice under high-LA TME (Fig. 3*D* and *SI Appendix*, Fig. S3*H*). Our data demonstrate that eEF1A2K408la promotes CRC cell proliferation both in vitro and in vivo.

Lactylation of eEF1A2 Mediates Enhanced Protein Synthesis in Cells. Since eEF1A2 is an essential GTPase responsible for recruiting aminoacyl-tRNA (aa-tRNA) to the ribosomal A-site during protein synthesis, we explored whether lactylation modulates its GTPase activity during translation elongation. We first purified wt-eEF1A2 and delac-eEF1A2 proteins from 293T cells in the presence of NaLa (*SI Appendix*, Fig. S3*I*) and subjected them to an in vitro guanosine triphosphate (GTP) hydrolysis assay. The velocity of phosphate formation catalyzed by eEF1A2 in the K408 lactylated state was almost equivalent to that in the delactylated state, indicating that K408 lactylation did not change the basal GTPase activity of eEF1A2 (Fig. 3*E* and *SI Appendix*, Fig. S3*J*). Notably, upon aa-tRNA stimulation, the catalytic efficiency of eEF1A2 was significantly higher in the K408 lactylated state as compared to the delactylated state (Fig. 3*E* and *SI Appendix*, Fig. S3*J*). These results suggest that eEF1A2 K408 lactylation increases its GTPase activity under aa-tRNA stimulation, which may boost translation elongation and thereby increases protein synthesis.

We then conducted a harringtonine run-off assay to measure the rate of transitional elongation in cells reconstituted with wt/delac-eEF1A2 (31, 32) (Fig. 3*F*). After treatment with harringtonine for 3 min, which blocked translation initiation, a 1.5-fold decrease in ribosome run-off was observed in delac-eEF1A2 overexpressing cells compared to the wt-eEF1A2 ones in the presence of NaLa (Fig. 3 *G*–*M*). These results emphasized the significance of eEF1A2K408la in maintaining elongation rates in tumor cells. To measured the protein synthesis efficacy in HCT116-sh eEF1A1/2 ±wt/delac-eEF1A2, we performed surface sensing of translation (SUnSET) assay (33). Depletion of eEF1A1 and eEF1A2 diminished protein synthesis in HCT116 cells (Fig. 3*N* and *SI Appendix*, Fig. S3*L*). Both wt-eEF1A2 and delac-eEF1A2 overexpression in eEF1A1/2-depleted cells moderately restored protein synthesis under normal culture conditions (*SI Appendix*, Fig. S3 *L* and *M*). Notably, cells reconstituted with wt-eEF1A2 exhibited more protein synthesis than the cells complemented with delac-eEF1A2 in the presence of NaLa (Fig. 3*N* and *SI Appendix*, Fig. S3*K*). To avoid potential biases associated with puromycylation approaches, we detected nascent protein synthesis by Click-iT reaction in cancer cells fed with amino acid (aa) analog L-homopropargylglycine (HPG) (34, 35). Compared to wt-eEF1A2 overexpressed cells, lower HPG incorporation in delac-eEF1A2 overexpressed cells was observed, indicating decreased protein synthesis caused by delactylation of eEF1A2 (Fig. 3*O* and *SI Appendix*, Fig. S3*N*). These data suggest that consistent with the oncogenic impact, eEF1A2K408la stimulates translation elongation and therefore enhances protein synthesis in CRC cells.

Identification of KAT8 as an eEF1A2 K408 Lactyltransferase. To identify the regulators of eEF1A2 lactylation, we performed immunoaffinity purification and subsequent LC–MS/MS in eEF1A2-overexpressed HCT116 cells for potential eEF1A2 interactors (Fig. 4*A* and Dataset S2). There are four eEF1A2 potential interactive acetryltransferases—DLAT, NAT10, NAA10, and KAT8—which could be the regulators of eEF1A2 lactylation. We overexpressed these four proteins, respectively, in HCT116 cells and validated their interactions with eEF1A2 (Fig. 4*B* and *SI Appendix*, Fig. S4*A*). IP analysis showed that compared to the control cells, the Kla level of eEF1A2 was significantly increased only in the KAT8-overexpressed cells, indicating that only KAT8 but not DLAT, NAT10, and NAA10 exhibited high Kla writer activity against eEF1A2 (Fig. 4*B* and *SI Appendix*, Fig. S4*A*). Moreover, knockdown of KAT8 markedly reduced the lactylation level of eEF1A2 (Fig. 4*C*). Co-IP analysis revealed a strong and specific association between KAT8 and endogenous eEF1A2 or exogenous Flag-tagged eEF1A2 but not eEF1A2 proteins harboring a K408R substitution (Fig. 4*D* and *SI Appendix*, Fig. S4*B*). The cytoplasmic colocalization of eEF1A2 and KAT8 in CRC cells further confirmed the interaction (*SI Appendix*, Fig. S4*C*). To investigate whether KAT8 directly transfers the lactyl group of lactyl-CoA to eEF1A2, we carried out an in vitro lactylation assay by incubating purified GST-eEF1A2/$eEF1A2_{K408R}$ and KAT8 in the presence of lactyl-CoA. A strong lactylation of GST-eEF1A2 but not GST-$eEF1A2_{K408R}$ was observed in the mixture of purified KAT8 and lactyl-CoA (Fig. 4*E*), indicating that KAT8 directly mediates eEF1A2 lactylation in K408.

Next, we examined whether KAT8 mediates eEF1A2 lactylation-enhanced protein synthesis and tumor growth. KAT8 was knocked-down in eEF1A1/2-depleted HCT116 cell overexpression of either

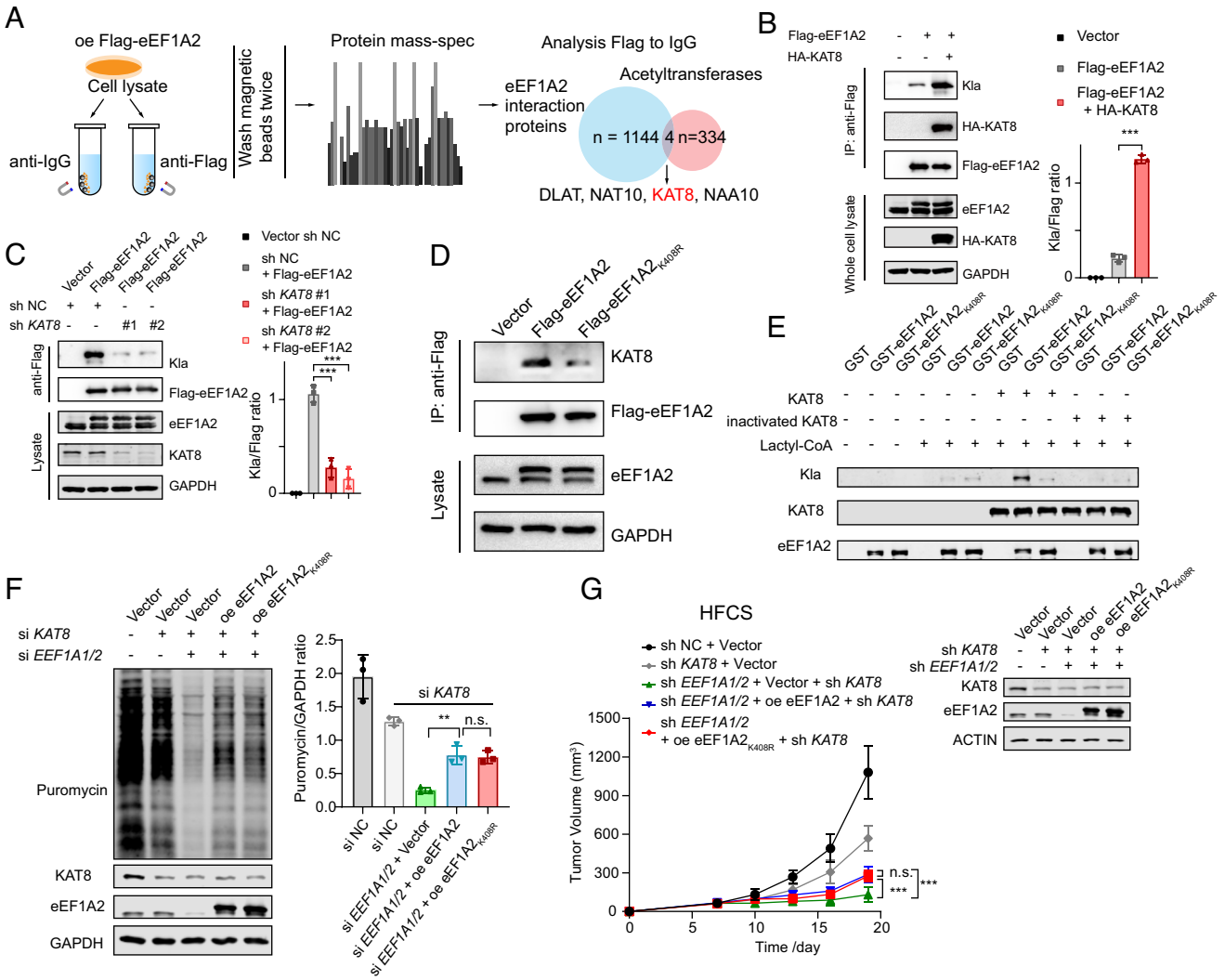

Fig. 4. Identification of KAT8 as an eEF1A2 K408 lactyltransferase. (*A*) Schematic diagram of identifying eEF1A2-interacting acetyltransferase using IP in combination with MS. (*B*) Kla levels of eEF1A2 in HCT116 cells transfected with indicated plasmids. The WCE were used for IP with an anti-Flag antibody, followed by WB for indicated targets. The *Right* panel represents WB quantification. (*C*) Kla levels of eEF1A2 in control vector or Flag-eEF1A2-overexpressed HCT116 cells transfected with scramble (sh NC) or KAT8-targted shRNAs. The WCE were used for IP with an anti-Flag antibody, followed by WB for indicated targets. The *Right* panel represents WB quantification. (*D*) Interaction between eEF1A2 and KAT8 in HCT116 stably expressing control vector or Flag-eEF1A2 or Flag-eEF1A2$_{K408R}$ was detected by Co-IP. (*E*) In vitro eEF1A2 lactylation assay. Purified GST-eEF1A2 or GST-eEF1A2$_{K408R}$ was incubated with recombinant KAT8 with or without lactyl-CoA. Kla levels of eEF1A2 were analyzed by WB. (*F*) Protein production levels were detected by SUnSET assays in control (sh NC plus control vector) or KAT8-depleted or eEF1A1/2-depleted HCT116 cells overexpressed with control vector or wt-eEF1A2 or delac-eEF1A2 in the presence of NaLa. The *Right* panel represents WB quantification. (*G*) Tumor growth curves for mice (n = 5/group) fed with HFCS bearing control (sh NC plus control vector) or KAT8-depleted or eEF1A1/2-depleted HCT116 cells overexpressed with control vector or wt-eEF1A2 or delac-eEF1A2. WB of WCEs with indicated antibodies was shown. $^{**}P < 0.01$; $^{***}P < 0.001$; n.s., no significance. Analyses were performed using unpaired, two-tailed Student's *t* test (*B*, *C*, and *F*) and two-way ANOVA (*G*). Data are shown as means ± SD.

wt or delac-eEF1A2. Depletion of KAT8 did not affect intracellular lactate levels of CRC cells (*SI Appendix*, Fig. S4*D*). However, KAT8 knock-down almost abolished the differences of protein synthesis efficacy between wt-eEF1A2 and delac-eEF1A2 expressing cells in the presence of NaLa (Fig. 4*F*). Correspondingly, the differences of enhanced tumor proliferation mediated by complementation of wt-eEF1A2 and delac-eEF1A2 both in vitro and in vivo was also attenuated after KAT8 depletion under high-LA TME (Fig. 4*G* and *SI Appendix*, Fig. S4*E*). KAT8 is thus a bona fide Kla transferase of eEF1A2.

KAT8 Is a Writer of Global Protein Lactylation. Whether eEF1A2 is the only KAT8 substrate or one of many substrates is unknown. We depleted KAT8 and observed substantially reduced Kla with unchanged lactate levels in CRC cells (Fig. 5 *A*–*C* and *SI Appendix*, Fig. S5 *A*–*D*). Although KAT8 has been recognized as an acetyltransferase (36), we found no obvious changes in lysine acetylation (Kac) levels in nonhistones after depleting KAT8 (*SI Appendix*, Fig. S5*E*). To map the responsible region for KAT8 acting as a Kla writer, we created three different HA-tagged truncated KAT8 which lacked the chromodomain (Δ1 to 121 aa), C2HC zinc fingers (Δ121 to 232 aa), and the enzymatic MYST domain (Δ232 to 458 aa), respectively (*SI Appendix*, Fig. S5*F*). We observed that both chromodomain (Δ1 to 121 aa) and C2HC zinc fingers (Δ121 to 232 aa) of KAT8 were dispensable for global protein lactylation, whereas the enzymatic MYST domain was necessary for its activity (Fig. 5*D*). In support of these observations, we found that MG149, which is an acetyltransferase inhibitor targeting the MYST domain of KAT8, decreased pan-Kla levels of CRC cells in a dose-dependent manner (Fig. 5*E* and *SI Appendix*, Fig. S5*G*). A moderate decrease of cellular Kla levels with the addition of A485, a catalytic inhibitor of p300, was observed, while the histone acetyltransferases (HAT) inhibitor-anacardic acid and the general control nonrepressed protein 5 (Gcn5)-related N-acetyltransferase inhibitor-remodelin hydrobromide showed not obvious Kla-regulatory effects in cells (Fig. 5*E*).

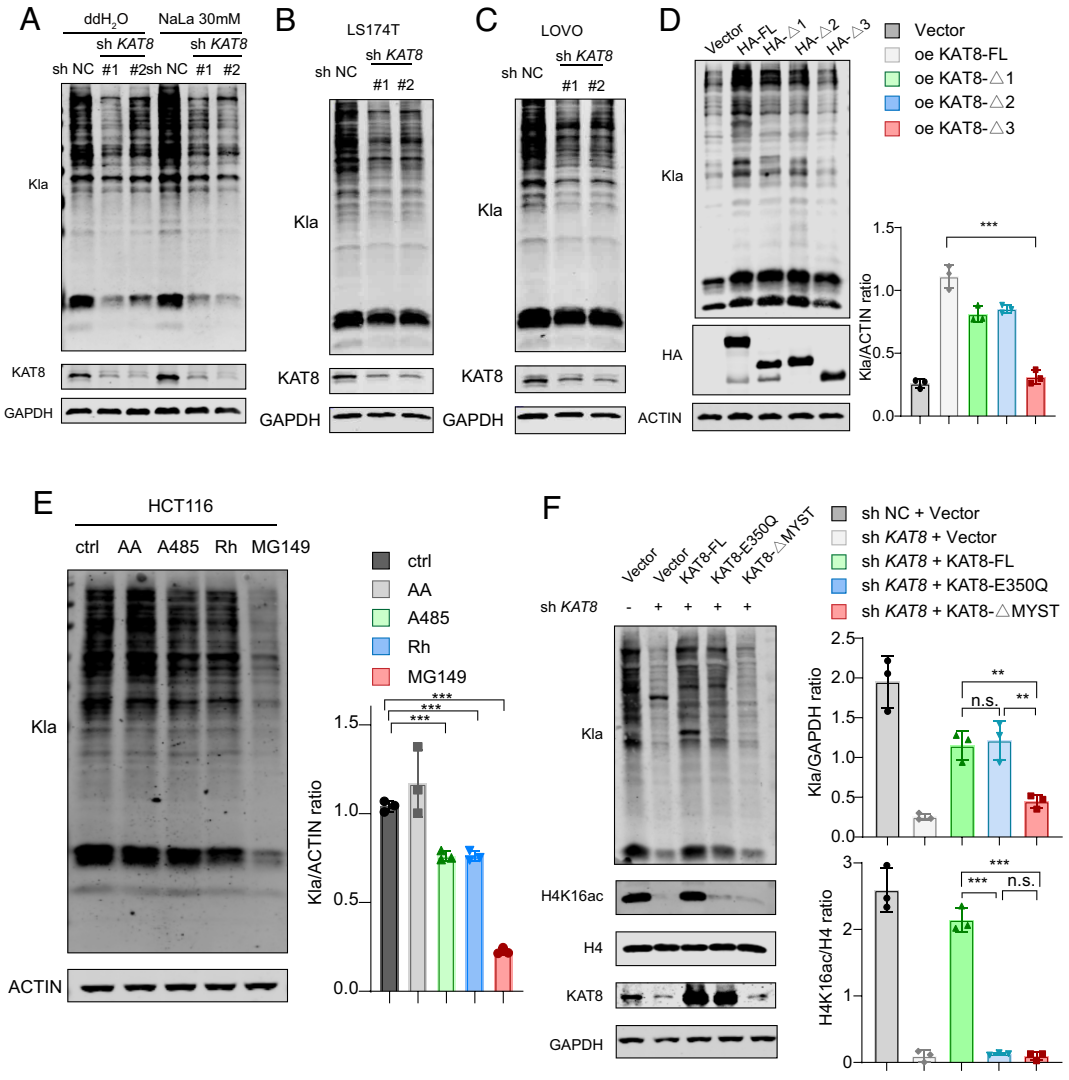

Fig. 5. KAT8 is recognized as a writer of global protein lactylation. (*A–F*) WBs. (*A*) Kla levels of HCT116 cells transfected with scramble (sh NC) or KAT8-targted shRNAs with or without NaLa. (*B*) Kla levels of LS174T cells transfected with scramble (sh NC) or KAT8-targted shRNAs. (*C*) Kla levels of LOVO cells transfected with scramble (sh NC) or KAT8-targted shRNAs. (*D*) Kla levels of control vector or HA-tagged KAT8 truncations-overexpressed HCT116 cells. The *Right* panel represents WB quantification. (*E*) Kla levels of HCT116 cells treated with different HAT inhibitors for 24h (AA, anacardic acid; Rh, remodelin hydrobromide). The *Right* panel represents WB quantification. (*F*) Kla and H4K16ac levels of control vector or HA-tagged KAT8 truncations-overexpressed HCT116 cells transfected with scramble (sh NC) or KAT8-targted shRNAs. The *Right* panel represents WB quantification. $^{**}P < 0.01$; $^{***}P < 0.001$; n.s., no significance. Analysis was performed using unpaired, two-tailed Student's *t* test (*D–F*). Data are shown as means ± SD.

Since KAT8 is a well-known HAT, it is important to differentiate its role as acetyltransferase vs. lactyltransferase in different contexts. We expressed wild-type KAT8 (wt-KAT8) or acetyltransferase catalytic dead (E350Q) KAT8 (ace-cdKAT8) in HCT116 cells, respectively. If the Kla changes mediated by KAT8 herein were dependent on its HAT activity, exogenous ace-cdKAT8 expression should not rescue the reduced Kla levels by KAT8-depleted cells. However, ace-cdKAT8 expression could still restore global Kla levels in KAT8-depleted cells, suggesting that lactyltransferase catalytic activity of KAT8 is independent of its property as a HAT (Fig. 5*F*).

It is reported that the acetylation of KAT8 is critical for its acetylating activity (37, 38). Since KAT8 could be acetylated and deacetylated by GCN5 and Sirtuin 6 (SIRT6), respectively (39), we regulated Kac levels of KAT8 by overexpressing GCN5 and SIRT6 in HCT116 cells and examined the subsequent changes of KAT8 lactylating capacity (*SI Appendix*, Fig. S5*H*). We found that the altered Kac levels of KAT8 did not result in changes of eEF1A2 Kla levels and pan-Kla levels (*SI Appendix*, Fig. S5*I*). Similar results were obtained by treating cells with inhibitors of GCN5 and SIRT6 respectively (*SI Appendix*, Fig. S5 *J* and *K*).

Global Landscape of KAT8-Regulated Lactylome in CRC Cells. To investigate KAT8-lactylated or acetylated proteins, we analyzed HCT116 cells with or without KAT8 depletion with LC–MS/MS (Fig. 6*A*) (25). We identified 8253 Kla sites on 2,390 proteins and 6,354 Kac sites on 2,613 proteins (*SI Appendix*, Fig. S6 *A* and *B*). Compared to control HCT116 cells, 1,483 Kla sites in 696 proteins and 42 Kac sites in 36 proteins were down-regulated and 67 Kla sites in 59 proteins and 758 Kac sites in 507 proteins were up-regulated in KAT8-depleted cells, respectively (Fig. 6*B*, *SI Appendix*, Fig. S6 *C* and *D*, and Dataset S3). These lactylome and acetylome data showed barely overlapping sites and proteins resulting from KAT8 depletion (*SI Appendix*, Fig. S6*D*). Furthermore, the amino acids flanking Kla or Kac sites exhibited significantly different patterns (Fig. 6*C* and *SI Appendix*, Fig. S6 *E* and *F*). The majority (390, 56%) of the lactylated proteins mediated by KAT8 had only one Kla site (Fig. 6*D*).

KAT8 has been reported to be a lysine acetyltransferase (KAT). We herein demonstrate a wider specificity for KAT8 as a writer of Kla. Therefore, proteins bearing down-regulated Kla sites in KAT8-depleted cells as compared with WT cells are more likely to be the direct lactylation targets of KAT8. Moreover, we found that KAT8 depletion did not decrease the protein expression level of p300, suggesting KAT8 regulated Kla independently of p300 (*SI Appendix*, Fig. S6*G*). To further validate KAT8-catalyzed Kla substrates, two KAT8-targeted proteins from the lactylomics, core binding factor β and cysteine and glycine-rich protein 1, were randomly selected for in vitro lactylation assays. Recombinant KAT8 directly lactylated these proteins in the presence of lactyl-CoA (*SI Appendix*, Fig. S6*H*).

Cellular distribution analysis revealed different subcellular localizations between KAT8-target Kla and Kac proteins (Fig. 6*E*).

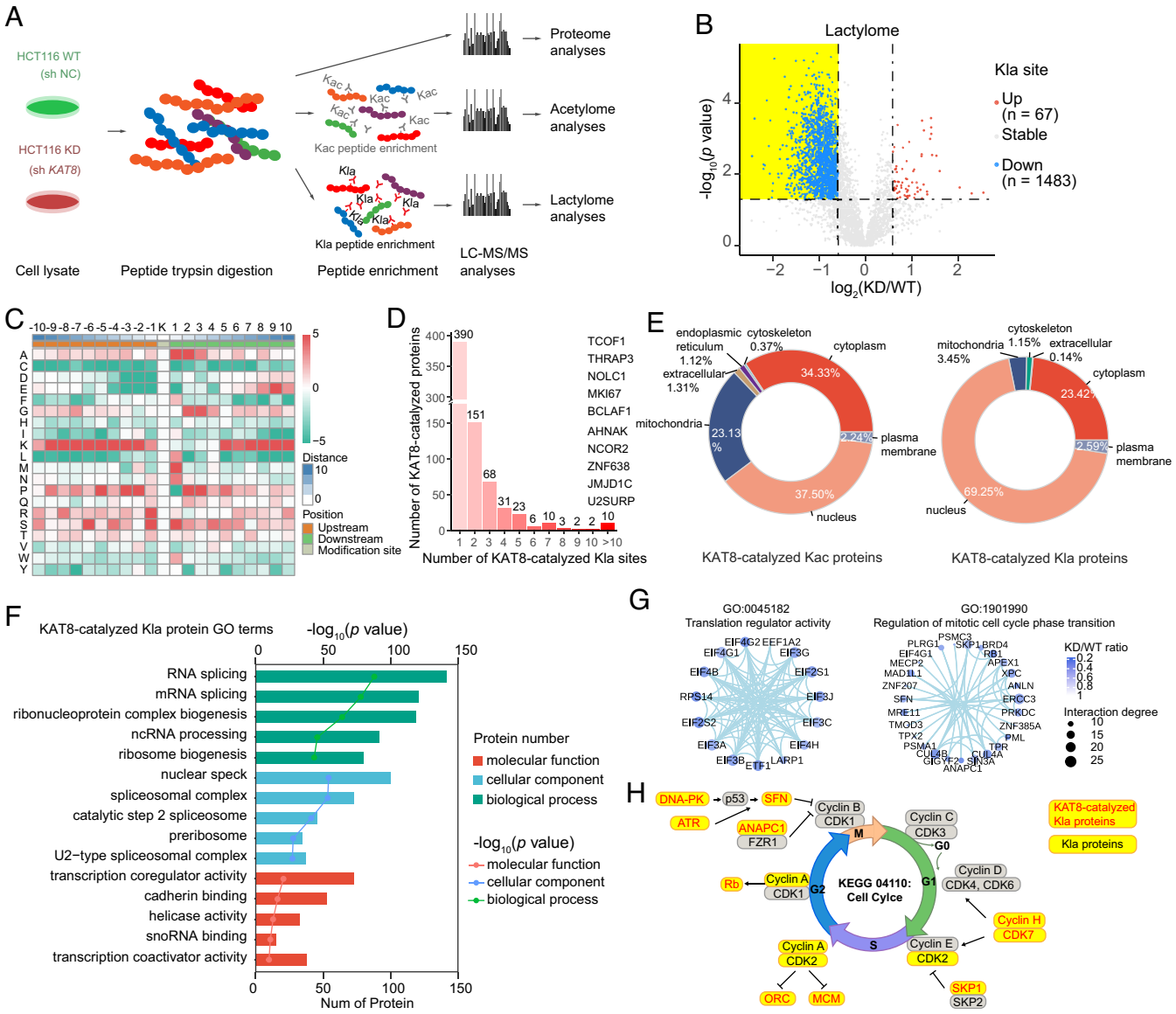

Fig. 6. Global landscape of the KAT8-regulated lactylome in CRC cells. (*A*) Schematic representation of the experimental workflow for identifying Kla and Kac substrates in HCT116 cells transfected with scramble (sh NC) or KAT8-targted shRNA. (*B*) Volcano plot showing the global lactylome changes in HCT116 cells transfected with KAT8-targted shRNA (KD) vs. cells transfected with scramble (WT). (*C*) Motif analysis of KAT8-catalyzed Kla-modified proteins. (*D*) Histogram of the number of KAT8-catalyzed Kla-modified sites per protein. Proteins with more than 10 sites of Kla are listed above the corresponding bar. (*E*) Donut charts showing the subcellular distribution of KAT8-catalyzed Kac-modified proteins (*Left*) and KAT8-catalyzed Kla-modified proteins (*Right*). (*F*) GO analysis associated with KAT8-catalyzed Kla-modified proteins. *P* values are derived from one-sided Fisher's exact test. (*G*) Protein–protein interaction network of KAT8-catalyzed Kla-modified proteins associated with translation regulator activity (*Left*) and regulation of mitotic cell cycle phase transition (*Right*) based on the STRING database. (*H*) Schematic of KAT8-catalyzed Kla-modified proteins (yellow box and red font) and Kla-modified proteins (yellow box) associated with cell cycle (KEGG:04110).

Correspondingly, Go and KEGG analysis showed distinct enrichments of the two PTMs (Fig. 6*F* and *SI Appendix*, Fig. S6 *I* and *J*). Many KAT8-lactylated proteins were involved in cancer-related GO terms such as translation regulator activity and regulation of mitotic phase transition and KEGG pathways including the cell cycle pathway and mismatch repair signaling (Fig. 6 *G* and *H* and *SI Appendix*, Fig. S6*K*). These data establish a potential functional link between KAT8-mediated lactylation and tumor development.

KAT8 Depletion Suppresses Tumor Growth in High-LA TME

To investigate the role of KAT8 in CRC, we analyzed the multiplexed IF staining of CRC TMA and the related patients' prognosis. We found a negative correlation between high KAT8 expression and OS of CRC patients, as well as a positive correlation between KAT8 expression and global Kla level in CRC tissues (Fig. 7 *A*–*C* and *SI Appendix*, Fig. S7*A*). In addition, depletion of KAT8 decreased Kla levels and attenuated proliferation of HCT116 cells, especially in high-LA culture conditions (Fig. 7 *D* and *E*). Similar results were obtained by treating HCT116 cells with MG149 (*SI Appendix*, Fig. S7 *B* and *C*). However, compared to normal cell culture conditions, high-LA culture conditions did not change the Kac level of KAT8 as well as the KAT8-acetylated capacity on histone H4 lysine 16 (*SI Appendix*, Fig. S7*D*). Together, these data suggest that KAT8-mediated Kla modification and corresponding potentiation of cellular proliferation are independent of its acetyltransferred mechanism.

We then assessed the role of KAT8 in tumorigenesis at different LA levels in vivo. Nude mice were subcutaneously injected with HCT116 cells with or without KAT8 depletion, followed by feeding with water or HFCS (*SI Appendix*, Fig. S7*E*). HFCS feeding

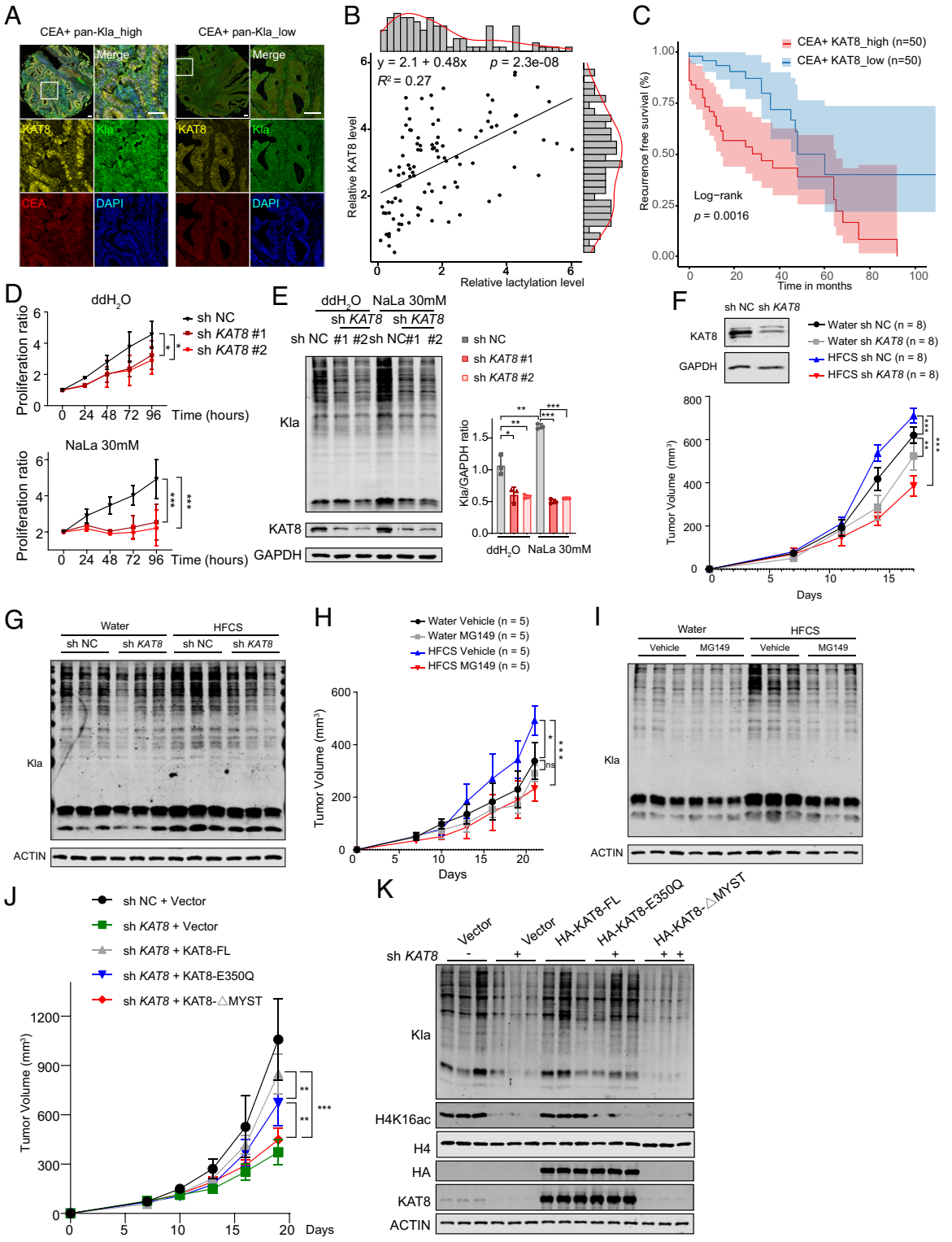

Fig. 7. KAT8 depletion suppresses tumor growth in high-LA TME. (*A*) Representative multiplexed immunostaining images of Kla and KAT8 in CRC. (Scale bars, 100 μm.) (*B*) Scatterplots depicting relative luminance intensity level between Kla and KAT8. The solid line in the scatterplot corresponds to the regression line (line of best fit). (*C*) Kaplan–Meier curves of time for recurrence-free survival showing the difference between CRC patients with low and high KAT8 levels. n = 100. (*D*) Cell proliferations of HCT116 cells transfected with scramble (sh NC) or KAT8-targted shRNAs with or without NaLa were measured with cell count proliferation assay. (*E*) Kla levels were detected in HCT116 cells transfected with scramble (sh NC) or KAT8-targted shRNAs with or without NaLa by WB. The *Right* panel represents WB quantification. (*F*) Tumor growth curves for mice (n = 8/group) fed with water or HFCS bearing HCT116 cells transfected with scramble (sh NC) or KAT8-targted shRNA. WB of WCEs with indicated antibodies was shown. (*G*) Representative Kla levels of mice bearing HCT116 cells transfected with scramble (sh NC) or KAT8-targted shRNA fed with water or HFCS. (*H*) Tumor growth curves for mice (n = 5/group) bearing HCT116 cells fed with water or HCFS and intraperitoneal injection (i.p.) administered with MG149 (2 mg/kg/day) or vehicle. (*I*) Representative tumoral Kla levels of mice bearing HCT116 cells fed with water or HCFS and i.p. administered with MG149 (2 mg/kg/day) or vehicle were detected by WB. (*J*) Tumor growth curves for mice (n = 5/group) bearing control vector or HA-tagged KAT8 truncations-overexpressed HCT116 cells transfected with scramble (sh NC) or KAT8-targted shRNA. (*K*) Representative tumoral Kla and H4K16ac levels were detected from mice bearing control vector or HA-tagged KAT8 truncations-overexpressed HCT116 cells transfected with scramble (sh NC) or KAT8-targted shRNA by WB. **P* < 0.05; ***P* < 0.01; ****P* < 0.001; n.s., no significance. Analyses were performed using unpaired, two-tailed Student's *t* test (*E*) and two-way ANOVA (*D*, *F*, *H*, and *J*). Data are shown as means ± SD.

but not KAT8 abundance altered tumoral lactate levels (*SI Appendix*, Fig. S7*F*). Compared to control cells, KAT8-depleted cells showed decreased tumor growth and reduced cancerous pan-Kla levels particularly in mice fed with HFCS (Fig. 7 *F* and *G*). Treatment with MG149 in tumor-bearing mice exhibited similar phenotypes (Fig. 7 *H* and *I* and *SI Appendix*, Fig. S7*G*). We then transfected full-length (wt-KAT8) or truncated KAT8 (ace-cdKAT8 or KAT8-ΔMYST) into KAT8-depleted HCT116 cells and compared cellular proliferation and tumorigenesis of these cells under high-LA conditions. Only KAT8-ΔMYST failed to restore proliferation and tumor growth of KAT8-deficient cells while wt-KAT8 and ace-cdKAT overexpression were capable to do so (Fig. 7*J* and *SI Appendix*, Fig. S7*H*). Consistently, complementation with wt-KAT8 and ace-cdKAT but not KAT8-ΔMYST increased global Kla levels in KAT8-deficient HCT116 (Fig. 7*K*). We thus infer that the lactyl-catalytic region of KAT8 locates within the MYST domain while is distinct from its well-known acetyl-catalyticdomain. Taken together, KAT8 is a lactyltransferase, which contributes to tumor development of CRC, especially in a high-LA TME.

Discussion

Being a metabolic product of the Warburg effect in cancer, lactate plays a pleiotropic role in tumorigenesis through metabolic rewiring and epigenetic modifications (13, 40). Lactylation is recognized as a PTM of histones derived from lactate. However, there are many open questions about lactylation including its occurrence on a broad range of proteins and functional consequences as well as its unknown regulators. We herein reveal that lactylation contributes to tumor development through promoting protein synthesis and identify KAT8 as a global lactylation transferase (*SI Appendix*, Fig. S8, Graphic Abstract).

Translation process requires a complex apparatus, composed of the ribosome, tRNAs, and various enzymes and translation factors (41). The crystal structure of the mammalian ribosomal elongation complex with aa-tRNA, eEF1A, and didemnin B (PDB:5LZS) shows that K408 of eEF1A2 could engage in a salt bridge interaction with the tRNA backbone and in return might affect the binding affinity of eEF1A2 to tRNA. We found that K408 lactylation of eEF1A2 is critical for enhancing ribosomal GTPase activity with aa-tRNA stimulation rather than affecting its basal hydrolysis efficacy. Combined with the structural analysis and our functional study, we inferred that the regulatory role of eEF1A2K408la on GTPase activity under tRNA stimulation could be relevant to the binding affinity between eEF1A2 and tRNA. The eEF1A2-tRNA binding affinity with or without K408 lactylation can be tested in a follow-up study. Considering that eEF1A2 were modified by various other PTMs such as methylation and phosphorylation (42, 43), it is of interest to unearth the cross talk between lactylation and other PTMs on eEF1A2 in regulating translation elongation.

Although the overall Kla levels in CRC are higher, there are some proteins sites with down-regulated lactylation observed in tumor tissues compared to normal tissues. GO analysis revealed that these down-regulated lactylated sites were mainly enriched in the MAPK pathway, cell migration, and apoptotic process. In the lactylation proteomics of other types of cancer such as hepatocellular carcinoma (9), there are also several protein sites with down-regulated lactylation in cancer tissues compared to normal tissues, which are mainly presented in metabolic pathways. Since the complicated impacts of lactylation on different protein sites cannot be simply generalized, further study is necessary to analyzed them under different situations.

KAT8 plays various roles in tumor development with its acetylation activity toward histones, manipulating oncogenes and tumor suppressor genes (44–46). In addition to its acetylation activity, we revealed an oncogenic role of KAT8 as a lactyltransferase. Our findings help elucidate the ambiguous role of KAT8 in cancer, indicating that the effect of KAT8 may be influenced by different lactate conditions of TME. Since cancer progression is an orchestrated process between cell-intrinsic signaling and TME, the functions of KAT8 in tumor should be interpreted in a context-dependent manner. We here identified that KAT8 contributed to tumor growth especially in high-LA TME. The underlying mechanism is related to the tumorigenic effects of eEF1A2K408la, but may also be associated with other KAT8-lactylated proteins, as many of them have been found to be enriched in oncogenic pathways. We speculate that the functional roles of KAT8-lactylated proteins could be amplified under high lactic conditions since such environment provides more lactate as donor for lactylation. The roles of these proteins deserve further explorations in specific contexts.

In summary, by presenting an initial report of global protein Kla modification in CRC, we revealed eEF1A2K408la as a functional hotspot to regulate translation elongation that contributes to tumorigenesis. Furthermore, we identified KAT8 as a pan-Kla writer and found KAT8-mediated Kla as a molecular mechanism to promote tumor growth. Our findings uncovered the widespread nature of Kla on nonhistone proteins in CRC and endow the regulation of Kla as a potential target with therapeutic value for cancer.

Materials and Methods

Ethics Statements. Human materials used in this study were approved by the Institutional Research Ethics Committee at The First Medical Center of PLA General Hospital. We obtained signed informed consents from all patients participating in the study. Animal experiments were approved by the Institutional Research Ethics Committee at The First Medical Center of the Chinese Academy of Medical Sciences Innovation Fund for Medical Sciences (ACUC-A02-2022-027 and ACUC-A02-2022-028).

Cell Culture and Treatment. NCM460, CCD841, CACO2, HCT116, SW480, LS174T, LOVO, and 293FT cells were obtained from the American Type Culture Collection. All cells were cultured in Dulbecco's Modified Eagle Medium (DMEM) medium supplemented with 10% FBS and maintained in a humidified atmosphere of 5% CO_2 at 37 °C. All cells used were cultivated for less than 30 passages and routinely tested negative for Mycoplasma by PCR.

Xenograft Models. The cell suspensions [1×10^6 cells per mouse, treated in PBS with MaxGel ECM at 1:1 (v/v)] were subcutaneously inoculated into the right flank of 5-wk-old female BALB/c nude mice. Tumor volumes were calculated by length × width^2 × 0.5 with a caliper every three days. When tumors reached the maximum allowed size, mice were killed and tumors were excised and snap-frozen.

Statistical Analyses. Unless otherwise specified, all experiments were conducted in three biologically independent replicates. Means and SD were plotted. Student's *t* test was used for statistical analyses. Two-way ANOVA was performed to cell proliferation assays and tumor growth curves. $^*P < 0.05$, $^{**}P < 0.01$, and $^{***}P < 0.001$ were considered statistically significant. Statistical details are included in figure legends. Data analyses including real-time mRNA expression, tumor-free, mouse-survival, tumor-burden, were performed using GraphPad Prism version 8.

Data, Materials, and Software Availability. All raw files and search results for MS of proteomics have been deposited in ProteomeXchange (RRID:SCR_004055) via iProX (www.iprox.org) with the identification no. PXD037744 (for ProteomeXchange) and IPX0005289000 (for iProX) (25). More details about experimental procedures and data analysis are provided in supporting Information.

ACKNOWLEDGMENTS. We acknowledge Prof. Benedikt Kessler from Oxford University for his generous help with English language editing throughout the manuscript. This work was supported by National Science and Technology Major Project (2021YFC2502000), Beijing Municipal Natural Science Foundation (Key program

Z220011), Haihe Laboratory of Cell Ecosystem Innovation Fund (22HHXBSS00012), National Natural Science Foundation of China (82273163, 82371640, 32100554, and T2225006), Chinese Academy of Medical Sciences Innovation Fund for Medical Sciences (CIFMS) (2021-1-I2M-018), and Beijing Nova Program.

Author affiliations: [a]Key Laboratory of Molecular Medicine and Biological Diagnosis and Treatment (Ministry of Industry and Information Technology), School of Life Science, Beijing Institute of Technology, Beijing 100081, China; [b]State Key Laboratory of Common Mechanism Research for Major Diseases, Haihe Laboratory of Cell Ecosystem, Department of Physiology, Institute of Basic Medical Sciences and School of Basic Medicine, Chinese Academy of Medical Sciences and Peking Union Medical College, Beijing 100005, China; [c]State Key Laboratory of Female Fertility Promotion, Center for Reproductive Medicine, Department of Obstetrics and Gynecology, Peking University Third Hospital, Beijing 10091, China; [d]National Clinical Research Center for Obstetrics and Gynecology, Peking University Third Hospital, Beijing 10091, China; [e]Department of General Surgery & Institute of General Surgery, the First Medical Center of Chinese People's Liberation Army General Hospital, Beijing 100583, China; [f]Department of Chemistry, University of Virginia, Charlottesville, VA 22904; [g]Department of Physiology, School of Life Science, China Medical University, Shenyang 110122, China; and [h]Faculty of Hepato-Biliary-Pancreatic Surgery, the First Medical Center of Chinese People's Liberation Army General Hospital, Beijing 100583, China

Author contributions: B.X., M.L., and Y.P. designed research; B.X., M.Z., J.L., P.Z., F.L., X.L., B.P., B.Z., Y.X., and Y.P. performed research; J.C., Y.W., W.D., and A.L. contributed new reagents/analytic tools; M.Z., J.L., and J.M. analyzed data; and H.Z., Y.X., M.L., and Y.P. wrote the paper.

1. D. Zhang *et al.*, Metabolic regulation of gene expression by histone lactylation. *Nature* **574**, 575–580 (2019).
2. R. A. Irizarry-Caro *et al.*, TLR signaling adapter BCAP regulates inflammatory to reparatory macrophage transition by promoting histone lactylation. *Proc. Natl. Acad. Sci. U.S.A.* **117**, 30628–30638 (2020).
3. J. Xiong *et al.*, Lactylation-driven METTL3-mediated RNA m(6)A modification promotes immunosuppression of tumor-infiltrating myeloid cells. *Mol. Cell* **82**, 1660–1677.e10 (2022).
4. L. Li *et al.*, Glis1 facilitates induction of pluripotency via an epigenome-metabolome-epigenome signalling cascade. *Nat. Metab.* **2**, 882–892 (2020).
5. H. Cui *et al.*, Lung myofibroblasts promote macrophage profibrotic activity through lactate-induced histone lactylation. *Am. J. Respir. Cell Mol. Biol.* **64**, 115–125 (2021).
6. K. Yang *et al.*, Lactate promotes macrophage HMGB1 lactylation, acetylation, and exosomal release in polymicrobial sepsis. *Cell Death Differ.* **29**, 133–146 (2022).
7. J. Yu *et al.*, Histone lactylation drives oncogenesis by facilitating m(6)A reader protein YTHDF2 expression in ocular melanoma. *Genome Biol.* **22**, 85 (2021).
8. N. Wan *et al.*, Cyclic immonium ion of lactyllysine reveals widespread lactylation in the human proteome. *Nat. Methods* **19**, 854–864 (2022).
9. Z. Yang *et al.*, Lactylome analysis suggests lactylation-dependent mechanisms of metabolic adaptation in hepatocellular carcinoma. *Nat. Metab.* **5**, 61–79 (2023).
10. C. Moreno-Yruela *et al.*, Class I histone deacetylases (HDAC1–3) are histone lysine delactylases. *Sci. Adv.* **8**, eabi6696 (2022).
11. Y. Zhang *et al.*, The function and mechanism of lactate and lactylation in tumor metabolism and microenvironment. *Genes Dis.* **10**, 2029–2037 (2023).
12. S. Walenta *et al.*, High lactate levels predict likelihood of metastases, tumor recurrence, and restricted patient survival in human cervical cancers. *Cancer Res.* **60**, 916–921 (2000).
13. W. Liu *et al.*, Lactate regulates cell cycle by remodelling the anaphase promoting complex. *Nature* **616**, 790–797 (2023).
14. M. Certo, C.-H. Tsai, V. Pucino, P.-C. Ho, C. Mauro, Lactate modulation of immune responses in inflammatory versus tumour microenvironments. *Nat. Rev. Immunol.* **21**, 151–161 (2021).
15. M. K. Mateyak, T. G. Kinzy, eEF1A: Thinking outside the ribosome. *J. Biol. Chem.* **285**, 21209–21213 (2010).
16. W. Abbas, A. Kumar, G. Herbein, The eEF1A proteins: At the crossroads of oncogenesis, apoptosis, and viral infections. *Front. Oncol.* **5**, 75 (2015).
17. A. Lamberti *et al.*, The translation elongation factor 1A in tumorigenesis, signal transduction and apoptosis: Review article. *Amino. Acids* **26**, 443–448 (2004).
18. J. Yang *et al.*, Effect of activation of the Akt/mTOR signaling pathway by EEF1A2 on the biological behavior of osteosarcoma. *Ann. Transl. Med.* **9**, 158 (2021).
19. A. Amiri *et al.*, eEF1A2 activates Akt and stimulates Akt-dependent actin remodeling, invasion and migration. *Oncogene* **26**, 3027–3040 (2007).
20. S. Liu *et al.*, METTL13 methylation of eEF1A increases translational output to promote tumorigenesis. *Cell* **176**, 491–504.e21 (2019).
21. C. B. Thompson *et al.*, A century of the Warburg effect. *Nat. Metab.* **5**, 1840–1843 (2023).
22. C. Chen *et al.*, Targeting LIN28B reprograms tumor glucose metabolism and acidic microenvironment to suppress cancer stemness and metastasis. *Oncogene* **38**, 4527–4539 (2019).
23. S. Liu *et al.*, Lactate promotes metastasis of normoxic colorectal cancer stem cells through PGC-1α-mediated oxidative phosphorylation. *Cell Death Dis.* **13**, 651 (2022).
24. Z. Tong *et al.*, Development of lactate-related gene signature and prediction of overall survival and chemosensitivity in patients with colorectal cancer. *Cancer Med.* **12**, 10105–10122 (2023).
25. B. Xie *et al.*, Lactylation contributes to colorectal carcinogenesis. Integrated Proteome Resources. https://www.iprox.cn//page/project.html?id=IPX0005289000. Accessed 27 October 2022.
26. C. von Mering *et al.*, STRING: A database of predicted functional associations between proteins. *Nucleic Acids Res.* **31**, 258–261 (2003).
27. T. Li *et al.*, Tumor suppression in the absence of p53-mediated cell-cycle arrest, apoptosis, and senescence. *Cell* **149**, 1269–1283 (2012).
28. J. Gao *et al.*, SIRT3 regulates clearance of apoptotic cardiomyocytes by deacetylating frataxin. *Circ. Res.* **133**, 631–647 (2023).
29. D. P. Waluk, F. Sucharski, L. Sipos, J. Silberring, M. C. Hunt, Reversible lysine acetylation regulates activity of human glycine N-acyltransferase-like 2 (hGLYATL2): Implications for production of glycine-conjugated signaling molecules. *J. Biol. Chem.* **287**, 16158–16167 (2012).
30. M. D. Goncalves *et al.*, High-fructose corn syrup enhances intestinal tumor growth in mice. *Science* **363**, 1345–1349 (2019).
31. T. Schneider-Poetsch *et al.*, Inhibition of eukaryotic translation elongation by cycloheximide and lactimidomycin. *Nat. Chem. Biol.* **6**, 209–217 (2010).
32. M. Fresno, A. Jimenez, D. Vazquez, Inhibition of translation in eukaryotic systems by harringtonine. *Eur. J. Biochem.* **72**, 323–330 (1977).
33. E. K. Schmidt, G. Clavarino, M. Ceppi, P. Pierre, SUnSET, a nonradioactive method to monitor protein synthesis. *Nat. Methods* **6**, 275–277 (2009).
34. M. Narita *et al.*, Spatial coupling of mTOR and autophagy augments secretory phenotypes. *Science* **332**, 966–970 (2011).
35. Y. Shen *et al.*, PQBP1 promotes translational elongation and regulates hippocampal mGluR-LTD by suppressing eEF2 phosphorylation. *Mol. Cell* **81**, 1425–1438.e10 (2021).
36. C. Pessoa Rodrigues *et al.*, Histone H4 lysine 16 acetylation controls central carbon metabolism and diet-induced obesity in mice. *Nat. Commun.* **12**, 6212 (2021).
37. M. Singh *et al.*, Histone acetyltransferase MOF orchestrates outcomes at the crossroad of oncogenesis, DNA damage response, proliferation, and stem cell development. *Mol. Cell Biol.* **40**, e00232-20 (2020).
38. Y. Xu, W. Wan, Acetylation in the regulation of autophagy. *Autophagy* **19**, 379–387 (2023).
39. B. Qiu *et al.*, KAT8 acetylation-controlled lipolysis affects the invasive and migratory potential of colorectal cancer cells. *Cell Death Dis.* **14**, 164 (2023).
40. C. Torrini *et al.*, Lactate is an epigenetic metabolite that drives survival in model systems of glioblastoma. *Mol. Cell* **82**, 3061–3076.e6 (2022).
41. S. Shao *et al.*, Decoding mammalian ribosome-mRNA states by translational GTPase complexes. *Cell* **167**, 1229–1240.e15 (2016).
42. M. B. Mendoza *et al.*, The elongation factor eEF1A2 controls translation and actin dynamics in dendritic spines. *Sci. Signal* **14**, eabf5594 (2021).
43. M. Piazzi *et al.*, eEF1A phosphorylation in the nucleus of insulin-stimulated C2C12 myoblasts: Ser^{53} is a novel substrate for protein kinase C βI. *Mol. Cell Proteomics* **9**, 2719–2728 (2010).
44. D. G. Valerio *et al.*, Histone acetyltransferase activity of MOF is required for MLL-AF9 leukemogenesis. *Cancer Res.* **77**, 1753–1762 (2017).
45. B. N. Sheikh, S. Guhathakurta, A. Akhtar, The non-specific lethal (NSL) complex at the crossroads of transcriptional control and cellular homeostasis. *EMBO Rep.* **20**, e47630 (2019).
46. A. Radzisheuskaya *et al.*, Complex-dependent histone acetyltransferase activity of KAT8 determines its role in transcription and cellular homeostasis. *Mol. Cell* **81**, 1749–1765.e8 (2021).